Developmental Biology 451 (2019) 167–179

Contents lists available at ScienceDirect

Developmental Biology

journal homepage: www.elsevier.com/locate/developmentalbiology

Lack of Cyclin B1 in zebrafish causes lengthening of G2 and M phases

Tetiana Petrachkova *, Laura A. Wortinger, Amber J. Bard, Jyotika Singh, Rachel M. Warga, Donald A. Kane

Department of Biological Sciences, Western Michigan University, Kalamazoo, MI, 49008, USA

ARTICLE INFO

Keywords:
Cyclin B
Cell cycle
G2/M transition
Mitosis promoting factor
Cell cycle progression

ABSTRACT

An essential part of the Mitosis Promoting Factor, Cyclin B1 is indispensable for cells to enter mitosis. We report here that the zebrafish early arrest mutant *specter* is a loss-of-function mutation in the *cyclin B1* gene. *cyclin B1* is maternally transcribed in zebrafish, and the zygotic phenotype is apparent by early segmentation. Lack of zygotic Cyclin B1 does not stop cells from dividing, rather it causes an abnormal and elongated progression through the G2 and M phases of the cell cycle. Many mutant cells show signs of chromosomal instability or enter apoptosis. Using CRISPR-mediated gene editing, we produced a more severe gain-of-function mutation confirming that *specter* is the result of nonfunctional Cyclin B1. Although also a recessive phenotype, this new mutation produces an alternative splice-form of *cyclin B1* mRNA, whose product lacks several key components for Cyclin B1, but not the Cdk1-binding domain. This mutant form of Cyclin B1 completely prevents cell division. We conclude that, although Cyclin B1 is critical for cells to enter mitosis, another cell cycle protein may be cooperating with Cdk1 at the G2/M checkpoint to sustain a partly functional Mitosis Promoting Factor.

1. Introduction

Cell cycle progression is regulated by conserved Cyclin-dependent kinases (Cdk) and cell cycle proteins (Cyclins). While Cdk's are constitutively expressed throughout the cell cycle, Cyclins are expressed more dynamically where they control individual phases of the cell cycle. Mammals and zebrafish have two types of Cyclin B (B1 and B2) (Minshull et al., 1989; Pines and Hunter, 1989). Chicken, frogs, flies, and worms also have a third type, Cyclin B3, essential for germline development (Gallant and Nigg, 1994; Kreutzer et al., 1995). Both Cyclin B1 and B2 are detectable in G1, rise through S phase and peak in late G2 or early M phase, after which they degrade in anaphase (Brandeis and Hunt, 1996). Cyclin B1 is primarily cytoplasmic but constantly shuttles between the nucleus and the cytoplasm in interphase, whereas Cyclin B2 is primarily in the cytoplasm during both interphase and mitosis (Jackman et al., 2003).

The G2 to M transition of the cell cycle relies predominantly on Cyclin B1 and Cdk1 activity (reviewed by J. Pines, 1995; Santamaría et al., 2007). To this end, Cyclin B1 has four major domains: a chromatin localization domain (CLD), essential for localization of Cyclin B1 to chromatin and the centrosomes (Pfaff and King, 2013); a destruction box (D-box), recognized by the anaphase promoting complex/cyclosome (APC/C) for Cyclin B1 ubiquitination during anaphase; a cytoplasmic retention domain (CRD), preventing Cyclin B1 from binding to the chromosomes prior to prophase; and a Cdk1-binding domain, essential for Cdk1 binding (Bentley et al., 2007; Draviam et al., 2001; Pfaff and King, 2013). Together with Cdk1, Cyclin B1 forms a protein kinase holoenzyme complex, also known as the Mitosis Promoting Factor (MPF) (Draetta et al., 1989). The MPF remains inactive until a Cyclin B1 threshold is surpassed in late G2 of the cell cycle (Allan and Clarke, 2007). Once DNA replication is complete, the MPF is activated through Cdc25 phosphorylation of inhibitory Wee1 and Myt1 kinases, to ensure that the MPF is fully activated (reviewed by Lindqvist et al., 2009). A high activity of the MPF allows cells to enter mitosis as the MPF translocates to the nucleus. Once in the nucleus, the MPF phosphorylates nuclear substrates, such as caspases, to protect mitotic cells against apoptosis (Ikegami et al., 1999; reviewed by Porter and Donoghue, 2003). The MPF also controls cell rounding in prophase (Gavet and Pines, 2010), and disassembly of the nuclear lamina in early prometaphase to promote nuclear envelope breakdown (reviewed by Nigg, 2001). Exit from mitosis is initiated by degradation of Cyclin B1 by the APC/C during mitosis (Clijsters et al., 2013; reviewed by Zachariae and Nasmyth, 1999). Cdk1 itself remains constitutively present to interact with other Cyclins (reviewed by Hochegger et al., 2008).

Cyclin B2 has been shown to be associated with the Golgi apparatus until prophase when the Golgi apparatus is targeted for disassembly

* Corresponding author.
E-mail address: tetiana.petrachkova@wmich.edu (T. Petrachkova).

https://doi.org/10.1016/j.ydbio.2019.03.014
Received 18 September 2018; Received in revised form 20 March 2019; Accepted 22 March 2019
Available online 28 March 2019
0012-1606/

mediated by Cyclin B2/Cdk1 (Draviam et al., 2001). Although not commonly believed to be important for the G2 to M transition, much like the "Maturation" Promoting Factor is for mitosis, Cyclin B2 is essential for oocyte "maturation". Together with the Hec1 kinetochore component, Cyclin B2 regulates microtubule nucleation during prophase and early prometaphase, as well as helps the centrosomes to organize the mitotic spindle in both mouse (Daldello et al., 2018; Gui and Homer, 2013; Li et al., 2018) and frog (Kotani et al., 2001).

In vivo studies show that mice lacking Cyclin B1 die *in utero*, whereas mice lacking Cyclin B2 are viable, only smaller than normal, and have reduced litter sizes (Brandeis et al., 1998). Flies lacking Cyclin B1 fail to form a spindle and cannot go through mitosis after the midblastula transition (Gong et al., 2010; Knoblich and Lehner, 1993; Nieduszynski et al., 2002). To date, however, there have been few studies that have examined the absence of functional Cyclin B1 during early development, except a recent study in mouse that showed that once the embryo runs out of maternal Cyclin B1, blastula cells arrest in G2 after the second division (Strauss et al., 2018). Despite this work on mouse Cyclin B1, other studies in human culture cells indicate that once Cyclin B1 is absent, Cyclin B2 enters the nucleus to form an activate MPF with Cdk1 overcoming the G2/M arrest (Bellanger et al., 2007; Gallant and Nigg, 1992). Therefore, there may be some redundancy in Cyclin B roles and differences between species.

Here we show that the zebrafish early arrest mutant *specter* (spr^{tu21}) is a recessive loss of function mutation in *cyclin B1*. We confirmed that spr^{tu21} is a mutation in *cyclin B1* using CRISPR/Cas9 mediated germline mutagenesis to create a new allele (spr^{ro1}), which fails to complement the original spr^{tu21} mutant allele. Like in other zebrafish cell cycle mutants (Kane et al., 1996; Riley et al., 2010; Song et al., 2004; Warga et al., 2016), once maternal *cyclin B1* mRNA is depleted, the zygotic phenotype is manifested. However, lack of zygotic *cyclin B1* mRNA does not appear to affect the embryo until quite late in development and rather than arresting the cell cycle, results in cells progressing through the cell cycle slower, delaying the G2 and M phases. Eventually, abnormal cell cycle progression causes numerous cellular changes, such as fewer and bigger cells, lagging chromosomes and cells that undergo apoptosis. spr^{ro1} mutant embryos exhibit a similar phenotype, only more severe and with an earlier onset. Further analysis indicated that in the *ro1* allele a Cyclin B1 product is made, but that it perhaps interferes with the function of the MPF. We conclude that while Cyclin B1 is critical for "normal" cell cycle progression, when it is absent there must be a compensatory mechanism that pushes cells through the G2/M checkpoint.

2. Material and methods

2.1. Mapping and genetic characterization

The *specter* (spr^{tu21}) mutation was isolated in the Tübingen screen (Haffter et al., 1996) and outcrossed to the polymorphic WIK (L5) strain of wild-type fish for mapping by half tetrad analysis (Johnson et al., 1995). Single stranded linked polymorphisms (Knapik et al., 1998), were used as in McFarland et al. (2005) to establish linkage. This mapped *specter* to one arm of Chromosome 5. Finer resolution on the Sanger map was further obtained using a haploid panel and the following microsatellite (z) markers:

z44961 (F 5′ GAG CAA TGT TTT CCC AGC AT 3′, R 5′ ATG GGC GGG ATT TAA TAA CC 3′); z7428 (F 5′ ATT GGG TGG TTG TGC ATT CT 3′, R 5′ CTG TCC AAT CTC GCT GTC AC 3′); z58519 (F 5′ CTT GCG GTT AAA CAT GCT TG 3′, R 5′ TTG TCT CCC TAG CGT GCT GT 3′); z65883 (F 5′ CCT TTG GGC TTT CTG ACA AG 3′, R 5′ GTG TTT GGT GAA TCA GCC CT 3′); z36189 (F 5′ TAA AAT CCT ACC GCG TAC CGG 3′, R 5′ GCA GGT GAA GGT GGA TGA AT 3′); z5538 (F 5′ TCA GCC ACA TTA GGG GAA AG 3′, R 5′ TTC AGA AGC CAT CCA TGT TG 3′); z3804 (F 5′ GCA TCT GGT GGT GTT GTA GG 3′, R 5′ CAG GAT CAA AAG CTG TGC AA 3′). This identified five potential candidate genes in a 4 Mb interval, one of which was *cyclin B1* (Supplementary Table 1). To determine whether spr^{tu21} was a mutation in *cyclin B1* we used RT-PCR and verified this by SANGER sequencing using genomic DNA from individual embryos.

2.2. Generating the spr^{ro1} mutant allele and identification of alternative splice variants

As described in Hwang et al. (2013) we constructed sgRNA targeted to the sequences GGCCAGGCGAGTGTTCTACT, a region complementary to a region in the intron 1 – exon 2 of the *cyclin B1* gene. Appropriate sense and antisense oligonucleotides were annealed together and subcloned into DR274 (Addgene) as per Hwang et al. (2013). To produce sgRNA, the vector was linearized by digestion with *Dra*I, and RNA was produced using the MAXIscript T7 kit (Life Technologies). *cas9* mRNA was generated using a Cas9 vector (Addgene) as per Hwang et al. (2013) using the mMESSAGE mMACHINE T7 ULTRA kit (Life Technologies).

To mutagenize fish, we injected wild-type embryos at concentrations from 9 to 13 pg of sgRNA together with 200 pg of *cas9* mRNA. The total number of embryos injected with CRISPR/Cas9 mRNA was approximately 1300 (Fig. 3B). After three months of growing mutagenized fish, only five survived. One was identified as a founder by complementation testing.

To identify alternative splice variants, total mRNA was extracted from phenotypic wild-type embryos from a transheterozygote cross and spr^{ro1} mutant embryos from a $spr^{+/ro1}$ cross. Reverse transcriptase PCR was performed using the following primer pairs: 5′ CCAGTTTGTTCATCGAGTCAC 3′ and 5′ GCAATCTCTGGTGGGTACATC 3′. Purified PCR products were then subcloned into pGEMT-Easy vectors (Promega) to generate enough DNA for SANGER sequencing.

2.3. Live cell cycle reporting and time-lapse microscopy

For analysis of the cell cycle in spr^{tu21} mutants, we bred the Dual FUCCI transgene (Bouldin and Kimelman, 2014) into the spr^{tu21} allele. Live anesthetized embryos were identified as mutant or wild type by their morphological phenotype, mounted at 24 h in 0.2% agarose and recorded in multi-plane every 6 minutes for 4 hours as previously described in Warga and Kane (2003), except we used a Nikon C2 confocal microscope, at 20x or 60x magnification, running NIS Elements Confocal software, in an imaging facility maintained at 30 °C during the recording.

For the analysis of the cell cycle in spr^{ro1} mutants, embryos derived from *ro1* heterozygotes were injected at the 1-cell stage with 25 pg *H2B-RFP* mRNA (Liu et al., 2017). Live embryos were mounted at 2-somites and recorded, as described above, every 5 minutes for 4 hours. At the end of the time-lapse, embryos were identified as mutant or wild type by their morphological phenotype.

Image processing and analysis was done using EOS Utility 2, Adobe Photoshop CS2, Adobe Photoshop 11.0, and NIS Elements Viewer (v. 4.20). During image processing, *H2B-RFP* labeled cells were pseudocolored from red to green.

2.4. Lineage tracing

Lineage tracing was adapted from those previously described (Warga and Nüsslein-Volhard, 1999; Warga et al., 2009). Briefly an individual blastomere was labeled between the 1 K- to 2 K–cell stages with a 5% solution of neutral rhodamine-dextran (10,000 MW). To count the number of enveloping layer cells, embryos were oriented in 3% methyl cellulose in Daniaeu's media and examined on a Zeiss Axioskop at: 40% epiboly, 60% epiboly, tailbud, 3-, 15-, and 18-somites and at 24 h. All embryos were re-examined at 24 h except in the case of 18-somites (18 h) and 24 h where embryos were also re-examined at 36 h.

2.5. In situ hybridization, BrdU labeling, antibody, and DAPI staining

Whole-mount RNA *in situ* hybridization was carried out using digoxigenin-labeled riboprobes following the protocol in Thisse and

Thisse (2008). For *cyclin B1 in situ* hybridization, embryos collected at 15-, 20-, and 24-h (Table 1), were first sorted by their morphological phenotype prior fixation before further characterization. BrdU pulse labeling was performed as described by Phillips et al. (2006) and stained with an anti-BrdU antibody (Abcam ab 1894, 1:1000). Whole-mount antibody staining was carried out using an anti-active Caspase 3 antibody (BD Biosciences, 1:200), an anti-alpha Tubulin antibody (Developmental Studies Hybridoma Bank, 1:25), an anti-GFP antibody (Santa Cruz, 1:500) or an anti-phospho-Histone H3 antibody (anti-pH3) (Santa Cruz, 1:1000) and detected with an AP-conjugated or peroxidase-conjugated secondary antibody (Santa Cruz, 1:1000) or Alexa Fluor 488-, 594-, 647-conjugated secondary antibodies (ThermoFisher Scientific, 1:200). DAPI staining was used at a concentration 1 ng/mL.

Embryos were cleared in 70% glycerol and photographed using a Sony F-707 digital camera or Canon T5 digital camera on a Zeiss Axioskop II, or a Nikon SMZU binocular stereomicroscope. In the case of fluorescent detection, we used a Nikon C2 Confocal microscope running NIS Elements Confocal software. Image processing was as described above.

3. Results

3.1. The spr mutant exhibits delayed development with ongoing apoptosis

The original *specter* (*spr*) allele was isolated in the Tübingen screen (Haffter et al., 1996) and identified in the early arrest group for phenotypes that displayed gross cellular abnormalities in the first 24 h of development (Kane et al., 1996). Represented by 2 Mendelian recessive lethal alleles (*tu21* and *ta214*), both were first distinguishable at 7-somites (12.5 h, Fig. 1A, A′) by a smaller head and tail compared to wild-type siblings. By 10-somites (14 h), mutant embryos were noticeably shorter, lacked clear somite boundaries, had smaller eye placodes, and the head and nervous system looked opaque. These defects increased over time so that by 20-somites (19 h), somite borders in the mutants were no longer distinguishable (Fig. 1B, B′) and by 30-somites (24 h), motor activity was abnormal.

Common characteristics for mutants that affect the cell cycle are loss of optical transparency, due to generalized cell death (Song et al., 2004; Warga et al., 2016), and for cells to be larger and fewer in number (Riley et al., 2010; Warga et al., 2016). We found that *spr* mutants had extensive apoptosis (Fig. 1C, C′), as revealed by antibody staining for the active form of Caspase-3 (Negron and Lockshin, 2004). Labeling of the blood cells by various markers showed that they were bigger and less numerous in the mutant (Fig. 1D-F′). Thus, *spr* mutants superficially resemble other cell cycle mutants.

3.2. spr is a mutation in cyclin B1

Initial mapping, using gynogenetic diploid embryos (Streisinger et al., 1986), linked spr^{tu21} to linkage group 5. Fine mapping of spr^{tu21}, using haploid embryos and seven microsatellite (z) markers narrowed it to a region between the markers z58519 and z65883 where no recombination was observed (Fig. 2A). These markers delineate approximately 85 genes including *cyclin B1* (Supplementary Table 1).

Based on the cell cycle phenotype, *cyclin B1* was the most promising candidate gene. Therefore, we sequenced mutant cDNA revealing a transition that caused a nonsense mutation (C139T; Fig. 2B) in exon 2 of the gene. This product, if transcribed, would result in a product lacking the Cdk1 binding domain, the destruction box, and the cytoplasmic retention domain – all critical for Cyclin B1 activity (Fig. 2C). *In situ* hybridization for the *cyclin B1* mRNA (Fig. 2D-G′) showed it was present in the two-cell embryo and maternal transcripts were maintained through early gastrulation (Fig. 2D and E). However, where in wild-type embryos *cyclin B1* is expressed throughout somitogenesis (Fig. 2F and G),

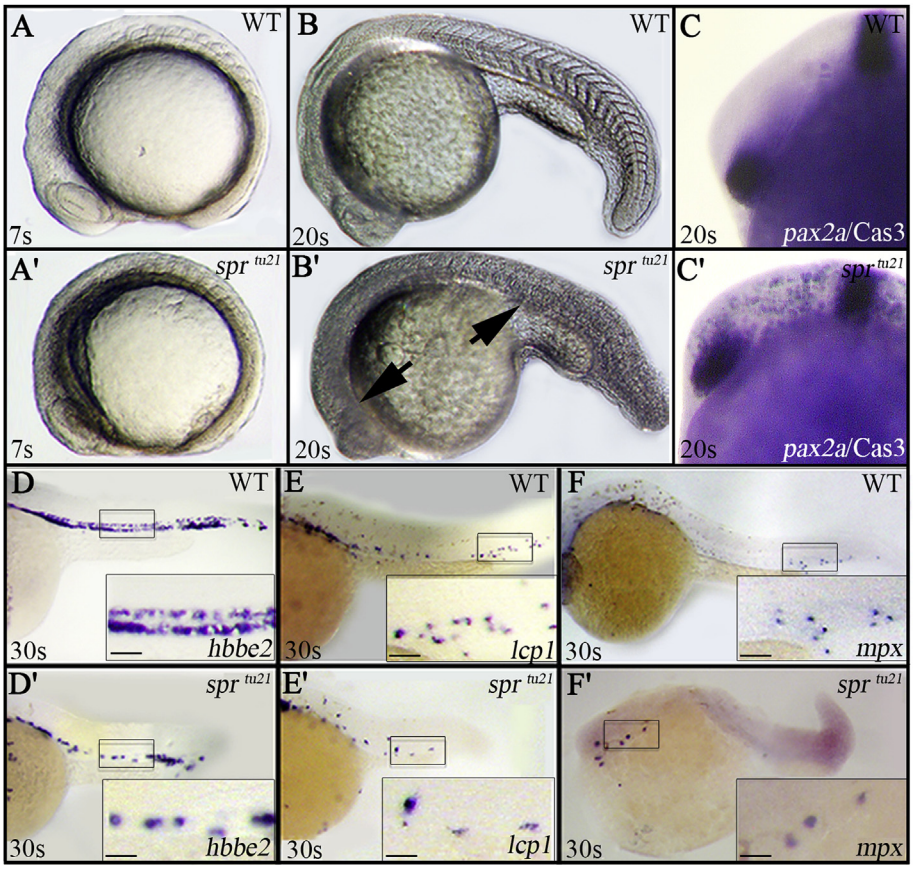

Fig. 1. The *spr* mutant phenotype. (A, B) Morphology of the live embryo, side view of: (A, B) wild-type and (A′, B′) spr^{tu21} embryos. Arrows indicate darkening in the head and trunk. Note the undefined somite borders in the mutant by 20-somites (19 h). (C, C′) Apoptosis, visualized by antibody staining for an active form of Caspase 3, is evident in the head of the *spr* mutant by 25-somites (21.5 h). Embryos are shown in side view using *pax2a* mRNA expression to define the area between the hindbrain and optic stalk. (D-F′) Blood cells are larger and less frequent in the *spr* mutant. (D, D′) Labeling of the blood by the erythrocyte marker, *hbbe2* (Brownlie et al., 1998), 8/8 mutants and 20/20 wild-type embryos displayed this phenotype; (E, E′) the macrophage marker, *lcp1* (Herbomel et al., 1999), 10/10 mutants and 17/17 wild-type embryos displayed this phenotype; (F, F′); and the neutrophil marker, *mpx* (Bennett et al., 2001; Lieschke et al., 2001), 10/10 mutants and 21/21 wild-type embryos displayed this phenotype. Boxes indicate the areas enlarged at higher magnification, scale bar is 20 μm.

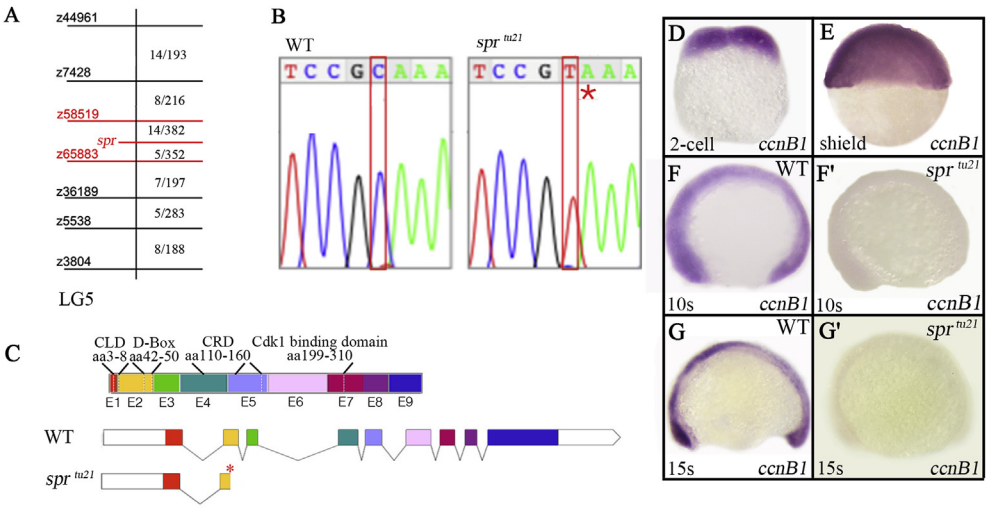

Fig. 2. Identification of *spr*^{tu21} as a mutation in *cyclin B1* gene. (A) A partial genetic map of Linkage Group 5 showing microsatellite (z) markers used in mapping on the left; and the number of recombinants in relation to the total number of individuals on the right. Combined haploid and diploid data show the least number of recombinants between the *specter* allele and z58519 and z65883, an interval that includes 85 genes (Supplementary Table 1). (B) Chromatograph sequence data showing the C139T transition that results in a premature stop codon (red asterisk). (C) Exon structure of the *cyclin B1* gene product showing 9 exons (E1-E9) and putative protein coding regions: chromatin localization domain (CLD), destruction box (D-box), cytoplasmic retention domain (CRD), and Cdk1-binding domain. The *spr*^{tu21} allele has a premature stop codon in exon 2 (red asterisk). (D-G′) *cyclin B1* mRNA is (D, E) maternally, and (F, G) zygotically expressed. (F′-G′) Note that expression of *cyclin B1* mRNA in the mutant embryo is significantly diminished at 10-somites (14 h) and absent by 15-somites (16.5 h).

in mutant embryos it is not (Fig. 2F′, G′). We interpret this to mean that this mutation likely produces a nonfunctional gene product that undergoes nonsense-mediated RNA decay. Thus by 10-somites (14 h), the embryo appears to have exhausted all maternal stores of *cyclin B1* transcripts.

3.3. Gene editing confirms that spr is a mutation in cyclin B1

To demonstrate that *spr*^{tu21} was a mutation in *cyclin B1*, we first attempted mRNA rescue using wild-type *cyclin B1*. Injecting *cyclin B1* mRNA into embryos derived from *tu21* heterozygotes at the 1-cell stage, did not alter the morphological phenotype of the mutant or its siblings. Further detection with antibody staining also did not reveal changes in mitosis or apoptosis. Undeterred, we changed strategy and edited the *cyclin B1* gene using CRISPR/Cas9. Our synthesized sgRNA had a recognition sequence in the second exon, 102 bp upstream of the mutation found in the *spr*^{tu21} allele (Fig. 3A). We identified *cyclin B1*-edited founders by complementation testing with *spr*^{tu21} heterozygotes (Fig. 3B). 10% of the progeny failed to complement, and the transheterozygote *spr*$^{tu21/ro1}$ embryos resembled the *spr*^{tu21} mutant phenotype (Fig. 3C–E), albeit more severe. Sequencing of *spr*^{ro1} mutant embryos showed that the edited sequence had a splice site mutation with a deletion of the *ag* acceptor splicing site and an insertion of four nucleotides (Fig. 3G). We conclude from these experiments that *spr* is caused by a mutation in *cyclin B1*.

3.4. The spr^{ro1} mutation possibly alters the Cyclin B1 protein

After outcrossing and recovering the *spr*^{ro1} allele, we found that like *spr*^{tu21}, it behaved as a Mendelian recessive lethal with no apparent dominant heterozygous phenotype. However, when homozygous it had an even more severe morphological phenotype than the null allele (Fig. 3C–F) suggesting it was a gain-of-function. We first asked if *cyclin B1* mRNA was expressed and found that *spr*^{ro1} mutants exhibited robust *cyclin B1* expression (Fig. 3F′) similar to that of wild-type embryos and very different from that seen in *spr*^{tu21} mutants (Fig. 3D′). By comparison, the *spr*$^{tu21/ro1}$ transheterozygote had an intermediate level of *cyclin B1* transcripts (Fig. 3E′). Therefore, *spr*^{ro1} mutants produce *cyclin B1* transcripts that do not undergo degradation.

To understand our *in situ* data, we first sorted embryos by wild type or mutant phenotype prior to fixation, followed by *in situ* hybridization, after which we sorted each category by the intensity of their *cyclin B1* expression (Table 1). We found that in a *spr*^{ro1} cross (Table 1), all embryos, both wild type (74% of the cross) and mutant (26% of the cross), had strong *cyclin B1* expression. However, in a *spr*^{tu21} cross (Table 1), not all wild-type embryos had strong *cyclin B1* expression (26% of the cross), as some had weaker expression (46% of the cross). In the quarter of the embryos that were mutant there was no expression (28% of the cross). This distribution correlates to the expected number of genotypic wild type, heterozygotes, and mutant. Thus, it would seem that if embryos inherit one copy of the *tu21* allele, whose transcript undergoes nonsense mediated decay, *cyclin B1* expression is less robust that normal. When we examined a transheterozygote cross (Table 1) we also found that not all wild-type embryos had strong *cyclin B1* expression (53% of the cross), as a portion of wild-type embryos exhibited weaker expression (24% of the cross), much like that of the transheterozygote mutant (23% of the cross). This distribution supports the idea that strong expression only happens when embryos do not inherit the *tu21* allele (all the wild type and half the heterozygotes). Altogether these results argue that intermediate expression is solely the result of the wild-type or *ro1* allele as the *tu21* allele has no detectable mRNA activity.

Further analysis revealed that *spr*^{ro1} mutants had many alternatively spliced mRNA products compared to the expected 741 bp product. This was demonstrated by extracting total mRNA from homozygous mutants and amplifying a fragment of the *cyclin B1* cDNA using a forward primer in the exon 1 and a reverse primer near the beginning of exon 6 (Fig. 4A). *spr*^{ro1} mutants had additional products of 900 bp and 1200 bp (Fig. 4A). Because embryos were sorted by their morphological phenotype, the wild-type pool also displayed these additional *ro1* products, although much fainter, as two thirds of these individuals were heterozygous. After subcloning these fragments into vectors, we also identified a further product of 250 bp (Fig. 4B) not seen earlier.

We cloned and sequenced a subset of these cDNAs, and found that most of them lead to out-of-frame transcripts with premature stop codons (Fig. 4C). Transcript 1 found a new (*ag*) acceptor site 4 nucleotides earlier than the original acceptor site, while transcript 2 found an acceptor site 48 nucleotides earlier than the original acceptor site. Both transcripts resulted in a frameshift mutation and a premature stop codon in exon 2. Transcript 3 retained intron 1, resulting in a premature stop codon in the retained intron.

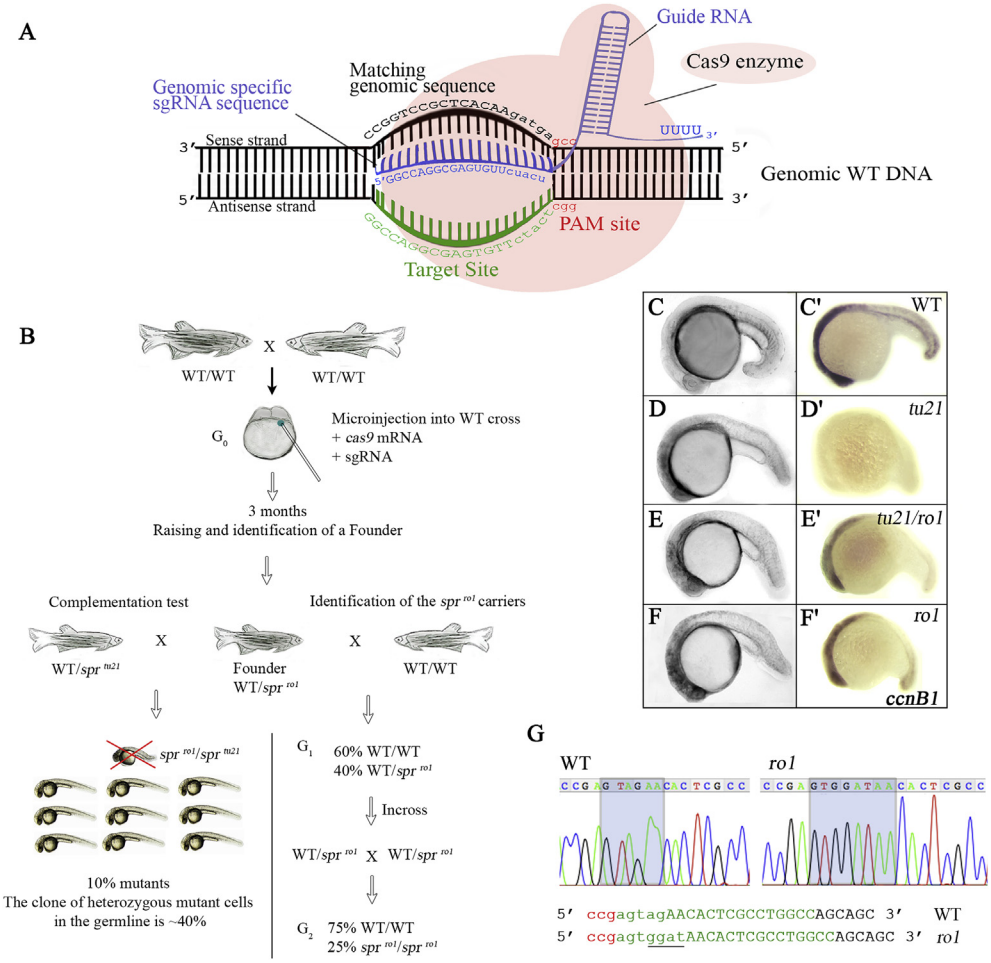

Fig. 3. CRISPR/Cas9-mediated mutagenesis confirms *spr*^{tu21} is a mutation in the *cyclin B1* gene. (A) Schematic representation of the CRISPR/Cas9 system, recognizing the target site within exon 2 of the *cyclin B1* gene. Blue, guide RNA (sgRNA); green, target site where *ag* is the acceptor site of intron 1; red, PAM site. (B) Diagram of CRISPR/Cas9-mediated mutagenesis. Embryos from a wild-type cross (G_0) were injected at the 2-cell stage with the *cas9* mRNA and sgRNA. After 3 months, founders were complementation tested to *spr*^{tu21} heterozygotes. In the G1, 10% of the eggs were *spr*$^{tu21/ro1}$ transheterozygotes suggesting that the germline clone was approximately 40% of the germline. After outcrossing the G1 *spr*^{ro1} founder to wild-type fish, identification of the *spr*^{ro1} carriers (G_2) was done by incrossing. (C–F) *In vivo* morphology and expression of *cyclin B1* mRNA in: (C′) wild-type, (D′) *spr*^{tu21}, (E′) *spr*$^{tu21/ro1}$, and (F′) *spr*^{ro1} mutant embryos at 25 h. All embryos are shown in side view. Note that the *spr*$^{tu21/ro1}$ (E′), and *spr*^{ro1} (F′) mutant embryos have zygotic *cyclin B1* mRNA transcripts at 20 h, but *spr*^{tu21} mutant embryos do not. (G) Chromatograph sequence showing a splice-site mutation occurs in the *spr*^{ro1}. The *spr*^{ro1} mutant has a 2-base deletion (AG acceptor site) and 4 base insertion (GGAT), underlined. Green, sgRNA target site; red, PAM site.

Table 1
Intensity of *cyclin B1* mRNA expression between 16 and 24 h.

specter cross	Phenotype	Strong (%)	Intermediate (%)	None (%)	Total embryos (%)
+/*tu21* x +/*tu21*	wild type[a]	26 (26%)	46 (46%)	0	100 (100%)[b]
	mutant[a]	0	0	28 (28%)	
+/*tu21* x +/*ro1*	wild type[a]	43 (53%)	20 (24%)	0	82 (100%)[c]
	mutant[a]	0	19 (23%)	0	
+/*ro1* x +/*ro1*	wild type[a]	118 (74%)	0	0	160 (100%)[d]
	mutant[a]	42 (26%)[e]	0	0	

[a] Statistically consistent with the Mendelian homozygous recessive segregation, using the chi square test.
[b] Embryos collected from four clutches in a +/*tu21* x +/*tu21* cross.
[c] Embryos collected from two clutches in a +/*tu21* x +/*ro1* cross.
[d] Embryos collected from four clutches in a +/*ro1* x +/*ro1* cross.
[e] *spr*^{ro1} mutants exhibited stronger *cyclin B1* expression compared to the transheterozygote but weaker than phenotypic wild type.

Transcript 4 however, had an alternative splicing variant where exon 2 through exon 5 were skipped, but remained in frame (Fig. 4C). This transcript possibly explains expression of *cyclin B1* in the *spr*^{ro1} mutant (Fig. 3F′) as it would not be degraded by nonsense-mediated degradation. If translated, transcript 4 would produce a protein with an expected size of 203 amino acids and would lack the destruction box, necessary for the protein targeted degradation in anaphase (Clute and Pines, 1999), but still retain a large portion of the Cdk1-binding domain. Thus, this product might interfere with other Cdk1-binding proteins and explain the more severe, gain-of-function phenotype.

3.5. The cell cycle is altered in specter mutants

Cyclin B has a well-characterized function in the G2/M transition as well as multiple roles during mitosis itself (reviewed by Pines, 1995; reviewed by Santamaría et al., 2007). To determine whether mutants of both alleles maintain a wild-type mitotic index, we first examined phospho-Histone H3 staining which labels the chromosomes from prophase to early anaphase (Hendzel et al., 1997) (Fig. 5A-A″). Counting the number of mitotic cells in rhombomere 4, outlined by expression of *egrb2* (*krox20*) in rhombomeres 3 and 5 (Oxtoby and Jowett, 1993), we found that the number of mitotic cells did not change between 7- and 20-somites (12 h and 19 h) in *spr*^{tu21} mutants, whereas in wild type it was increasing (Fig. 5B). However, at 25-somites (21.5 h), the number of mitotic cells was significantly lower, compared to wild-type (Fig. 5B). In contrast, the number of mitotic cells in *spr*^{ro1} mutants was already significantly diminished by 7-somites and continued to decline between 7- to 25-somites (12–21.5 h) (Fig. 5B). Taking into account the more

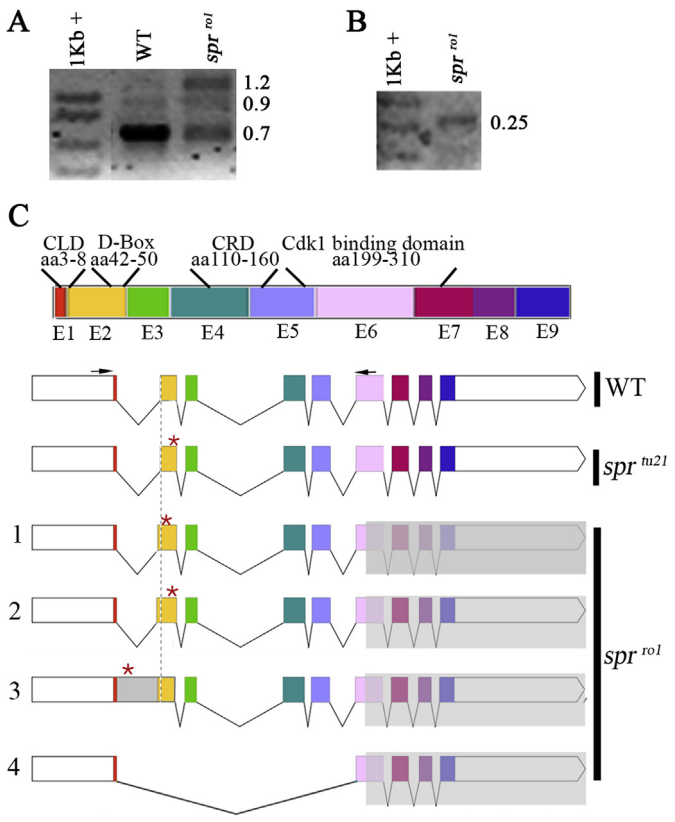

Fig. 4. The *spr*^{ro1} mutant has alternative splice variants. (A) Selection of *cyclin B1* transcripts in wild-type and *spr*^{ro1} mutant embryos at 30 h. *spr*^{ro1} mutants have additional transcription products. The expected product size is 741 bp (PCR product produced by a forward primer in the 5′UTR and a reverse primer in exon 6), but *spr*^{ro1} mutants also have a 900 bp and 1200 bp product. Extra products seen in a pool of wild-type siblings are much weaker and result from heterozygous individuals that are phenotypically wild-type. (B) Additional *cyclin B1* transcript found after cloning into the pGEM-T Easy vector. The 255 bp product amplified using the T7 and SP6 primers is an alternatively spliced *cyclin B1* mRNA (cDNA) product. (C) Splice site map of the *cyclin B1* gene in wild-type, *spr*^{tu21}, and *spr*^{ro1} (1–4). Primers used are marked on the wild-type schematic with black arrows, the expected cDNA product is 741 bp. Grey box is the part of the transcript that was not amplified in the PCR reaction. A red asterisk indicates introduced stop codons. The dashed line indicates the beginning of E2 (yellow) to help visualize additional nucleotides. *spr*^{ro1} mutants have at least four alternative splice site variants: (1) acceptor site in intron 1 is 4 nucleotides upstream of the original acceptor site (−4) followed by a stop codon in the E2; (2) acceptor site in intron 1 is 48 nucleotides upstream of the original acceptor site (−48) followed by a stop codon in E2; (3) intron retention splice variant, with premature stop codon +132 bp of the intron; and (4) In-frame splice site, where the first acceptor site is in intron 5, skipping E2-E5.

severe phenotype (Fig. 3F′) and a possible dominant effect of the gain-of-function *ro1* allele, we more carefully examined the number of mitotic cells in their phenotypically wild-type siblings (60 embryos from 3 different clutches). There was no significant difference among the wild-type group, supporting that *ro1* behaves as a recessive allele. Likewise, anti-pH3 staining reveals that neural cells normally undergo division at the midline in phenotypically wild-type siblings (Fig. 5A, arrow), however neither of the mutants exhibited this behavior. Instead, cells in the *spr*^{tu21} mutant seem to divide after they leave the midline and cells in *spr*^{ro1} do not divide at all.

We initially hypothesized that the pH3-positive cells at the earlier stages in *spr*^{tu21} mutants were the same cells at later stages of development, arrested in the G2/M transition. To determine if this were so, we used the Dual Fluorescent Ubiquitination Cell-Cycle Indicator (FUCCI) (Abe et al., 2013; Sugimoto et al., 2004; Sugiyama et al., 2009). This construct takes advantage of the oscillating levels of Cdt1, which accumulates during G1 phase, and Geminin, which accumulates during S, G2, and early M phase, to report the stage of the cell cycle. In zebrafish, a single transgene expresses mCherry under the control of a Cdt1-degron, and Cerulean under the control of a Geminin-degron (Bouldin and Kimelman, 2014). We hypothesized that if cells stopped dividing in mutant embryos, they would be arrested in the G2 and early M (blue) phases of the cell cycle in mutant embryos. In wild-type embryos, cells were predominantly in the G1 (red) phase of the cell cycle (Fig. 5C-C″). In contrast, in both *spr*^{tu21} (Fig. 5D-D″) and *spr*$^{tu21/ro1}$ (Fig. 5E-E″) mutant embryos cells were predominantly in the S, G2, or early M (blue) phase of the cell cycle. This suggests a possible cell cycle arrest. When cells were in G1, their morphology was altered compared to wild type (Fig. 5C, D, E): not only were nuclei bigger, indicative of endoreplication, but many were pyknotic suggesting that these cells were undergoing apoptosis.

3.6. Cells in *spr*^{tu21} mutants continue to slowly divide

To determine if cells really stop dividing, we labeled single cells in the mid-blastula with lineage tracer dye and followed divisions in the enveloping layer (EVL) (Fig. 6A). Unlike the deep cells, EVL cells tend to survive in both mutant alleles, perhaps because they divide less frequently. Cell cycle mutants typically do not exhibit their phenotypes until maternal transcripts are depleted (Kane et al., 1996; Unhavaithaya et al., 2013; Warga et al., 2016), therefore we waited to examine embryos until 30% epiboly (4.66 h), a few hours after zygotic transcription begins.

We found that constant UV light caused high amounts of cell death in *spr* mutants, compared to wild-type siblings, thus, we only examined clones intermittently no more than three times selecting an early time-point (between 30% epiboly to mid-somites) and a later time-point (24 h and/or 36 h of development) (Fig. 6B). Surprisingly, we found that the cells in the *spr*^{tu21} mutant did not stop dividing during the observed period. However, in the *spr*^{ro1} allele, there were no cell divisions after tailbud.

To determine if the reason EVL cells in the *spr*^{tu21} mutant have fewer divisions is that their cell cycle is longer than cells in wild-type, we recorded embryos, using the Dual FUCCI transgene (Fig. 6C, Supplementary Movie 1, Movie 2) beginning at 24 h of development, when maternal products are presumably exhausted (Fig. 2D′). Because the cell cycle at this stage takes approximately 8 h (Siefert et al., 2015), we recorded embryos for 10 h and limited UV damage by not using the mCherry-Cdt1 signal. We found that EVL cells in the wild type spent an average of 21.7 ± 4.1 min in mid-M to S phase (from the loss of the Cerulean-Geminin signal to regaining it in the daughter cells), whereas EVL cells in the *spr*^{tu21} mutant spent an average of 55.2 ± 11.0 min in the same stage of the cell cycle ($p < 0.05$). Hence, *spr*^{tu21} mutant cells spent more time in mitosis.

Supplementary video related to this article can be found at https://doi.org/10.1016/j.ydbio.2019.03.014.

Although EVL cells no longer divide after tailbud in the *spr*^{ro1} mutant (Fig. 6B), we did not know whether deep cells, which give rise to the embryos proper (Kimmel et al., 1990), cease to divide. To this end, we injected *H2B-RFP* mRNA at the 1-cell stage and then recorded embryos beginning at 2-somites (10.5 h). As the cell cycle at this earlier stage is approximately from 4 to 5 h (Kimmel et al., 1994; Siefert et al., 2015), (Fig. 6D, Supplementary Movie 3, Movie 4), we only recorded embryos for 4.5 h. We observed 25 divisions in a wild-type sibling embryo during this period, but only 8 in the mutant. Most mutant cell divisions occurred during the first hour of recording, the last division being recorded at 5-somites (11.7 h) (Fig. 6D). Notably, this final cell spent far longer time in metaphase than normal, much like *spr*^{tu21} EVL cells do later (Fig. 6C, Supplementary Movie 1, Movie 2). Hence, this demonstrates that *spr*^{ro1} mutants also exhibit an increased period spent in M phase.

Supplementary video related to this article can be found at https://

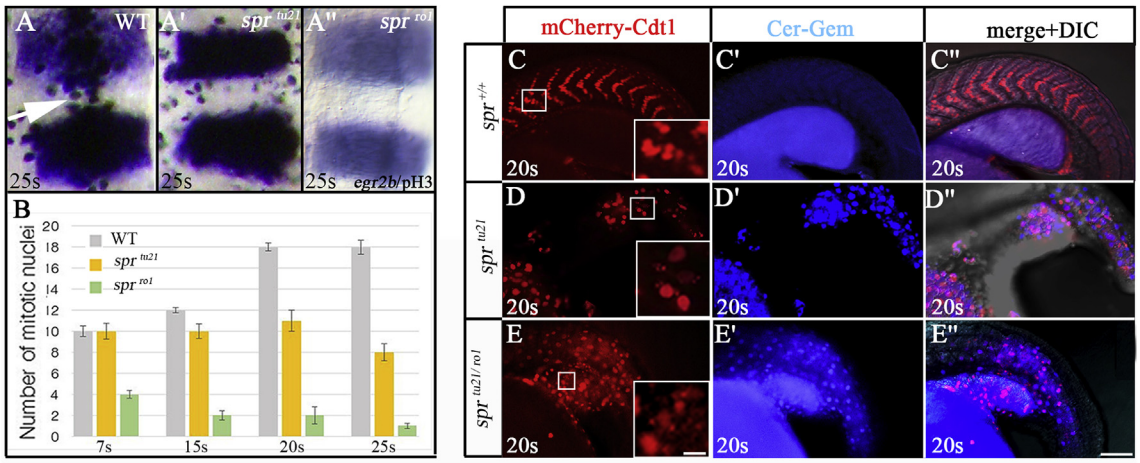

Fig. 5. Cyclin B1 mutants have an abnormal cell cycle progression. (A-A″) anti-pH3 staining shows *spr* mutants have fewer cells in mitosis between the *egr2b* stripes in rhombomeres 3 and 5, dorsal view. Mitotic cells align at the dorsal midline (white arrow) in the wild-type embryo (A), but do not in the spr^{tu21} mutant (A′) whose mitotic cells are irregularly shaped. In the spr^{ro1} mutant (A″), pH3 staining is weak and reveals few mitotic cells. (B) Quantification of the number of mitotic cells between the *egr2b* stripes in the wild-type embryos (grey), spr^{tu21} mutant (yellow), and spr^{ro1} mutant (green) between 7- and 25-somites (12 h and 21.5 h). Starting at 15-somites (16.5 h), the number of mitotic cells in the spr^{tu21} allele is significantly fewer ($p < 0.05$) compared to wild-type embryos. The counts for the spr^{ro1} allele are statistically significant compared to both, wild-type and spr^{tu21} at all stages ($p < 0.01$). (C-E″) The Dual FUCCI transgene shows that cells in the *spr* mutant reside in the wrong phase of the cell cycle at 20-somites. Shown are populations of cells in the tail where the cell cycle reporter mCherry-Cdt1 (red) defines cells in G1 (G0) stage (C–E) and the Cerulean-Geminin (blue) defines cells in S/G2/early M stages (C′-D″). Whereas the majority of cells in wild-type embryos are in the G1 (G0) stage of cell cycle (C-C″), the majority of cells in spr^{tu21} (D-D″) and $spr^{tu21/ro1}$ (E-E″) mutants are in the S/G2/early M phase of the cell cycle. Scale bar is 100 μm. Inserts show that G1 (G0) cells have abnormal shapes in mutant embryos, scale bar is 10 μm.

doi.org/10.1016/j.ydbio.2019.03.014.

3.7. spr^{tu21} mutant cells have a longer G2 phase

To establish if the G2 phase of the cell cycle was also lengthened, we labeled wild-type and spr^{tu21} embryos at 24 h with BrdU for 1 hour. Afterwards, we stained with an anti-BrdU antibody to label cells in the S phase of cell cycle, an anti-GFP antibody to label cells in S through early M (the Cerulean-Geminin signal), and an anti-pH3 antibody to label cells in mitosis (Fig. 7A-B‴). To analyze these results, we counted cells positive for these markers in different combinations to distinguish between cell cycle phases (Fig. 7C). Our data showed that: first, there were significantly more wild-type cells positive for only BrdU (S phase), and BrdU with other markers (S→M; S→G2→M; S→M) than those in the mutants. Second, there were significantly fewer wild-type cells positive for only Geminin (G2 phase) and Geminin with anti-pH3 (G2→M) than those in the mutants. Third, there was no significant difference between the number of cells positive for only anti-pH3 (M phase).

In summary, we found a population of cells in spr^{tu21} mutants that can go through a new cell cycle like wild-type cells, even at 24 h. However, there were fewer cells that phased from S to G2 or to M, as the majority of the mutant cells were in the G2 phase and G2/M transition compared to their wild-type siblings.

Although cells in the spr^{tu21} loss-of-function allele remain mostly in the G2/M phase of the cell cycle, altogether, these results show that cells are not arrested, rather they just spend far longer in G2 and M phases. Therefore, lack of zygotic Cyclin B1 does not prevent cells from dividing, it simply slows them down.

3.8. *spr* mutant cells exhibit signs of chromosomal instability

One of the functions of an active MPF is to control chromosome condensation (Kimura et al., 1998) and microtubule dynamics during mitosis. To further investigate why mutant cells do not go through mitosis as fast as wild-type cells, we examined their chromosomes and microtubules more closely using DAPI nuclear staining and an anti-alpha Tubulin antibody at 24 h concentrating on deep cells derivatives (Fig. 8), which we know still divide, at least in the tail of the spr^{tu21} mutant (Fig. 6D, Supplementary Movie 2). Ordinarily, microtubules ensure a correct and equal segregation of chromosomal content in the two daughter cells (Fig. 8A-A″). In spr^{tu21} mutants, there was no difference in chromatin condensation at mitotic entry. However, we saw abnormalities in many mutant cells during anaphase and telophase (Fig. 8B-D″). While some cells separated their genetic material normally, others had an abnormal microtubule organization where astral microtubules were absent and the central spindle microtubules were hyper aggregated (Fig. 8B′, B″). In addition, some cells had microtubules attachment errors, resulting in lagging chromosomes (Fig. 8C-C″) or chromatin bridges (Fig. 8D-D″). We also observed pyknotic nuclei (Fig. 8E-E″) having the typical apoptotic microtubule network described by Moss et al. (2006) that are thought the result of genomic instability and aneuploidy.

Surprisingly, even in the $spr^{tu21/ro1}$ and spr^{ro1} mutants, divisions at 24 h still occurred (Fig. 8F-J″), although these were few and predominantly in ventral epidermal cells, and not the tail. As above, some cells in telophase, appeared normal (Fig. 8F-F″), suggesting a successful division. Yet, like the null mutant, there were cells in telophase with over bundled astral and central microtubules (Fig. 8G′, H′, I′, J′), microtubule attachment errors with lagging chromosomes (Fig. 8G, H, J), as well as pyknotic nuclei (Fig. 8F, red arrowhead). Overall however, microtubule organization was more disrupted in the spr^{ro1} mutant cells, including highly concentrated and unfocused microtubules at the onset of anaphase with abnormal spindle orientations (Fig. 8I–I″). Notably this latter phenotype was also observed in the $spr^{tu21/ro1}$ mutant, only not as severe, but never in the spr^{tu21} mutant (data not shown). These data suggest that in the absence of a wild-type Cyclin B1 product, the gene product from even one *ro1* allele is enough to prevent a compensatory mechanism for sustaining normal cell division.

4. Discussion

As a gateway to mitosis, Cyclin B1 and Cdk1 play an essential role in cell cycle progression. However, their role is not fully understood in early

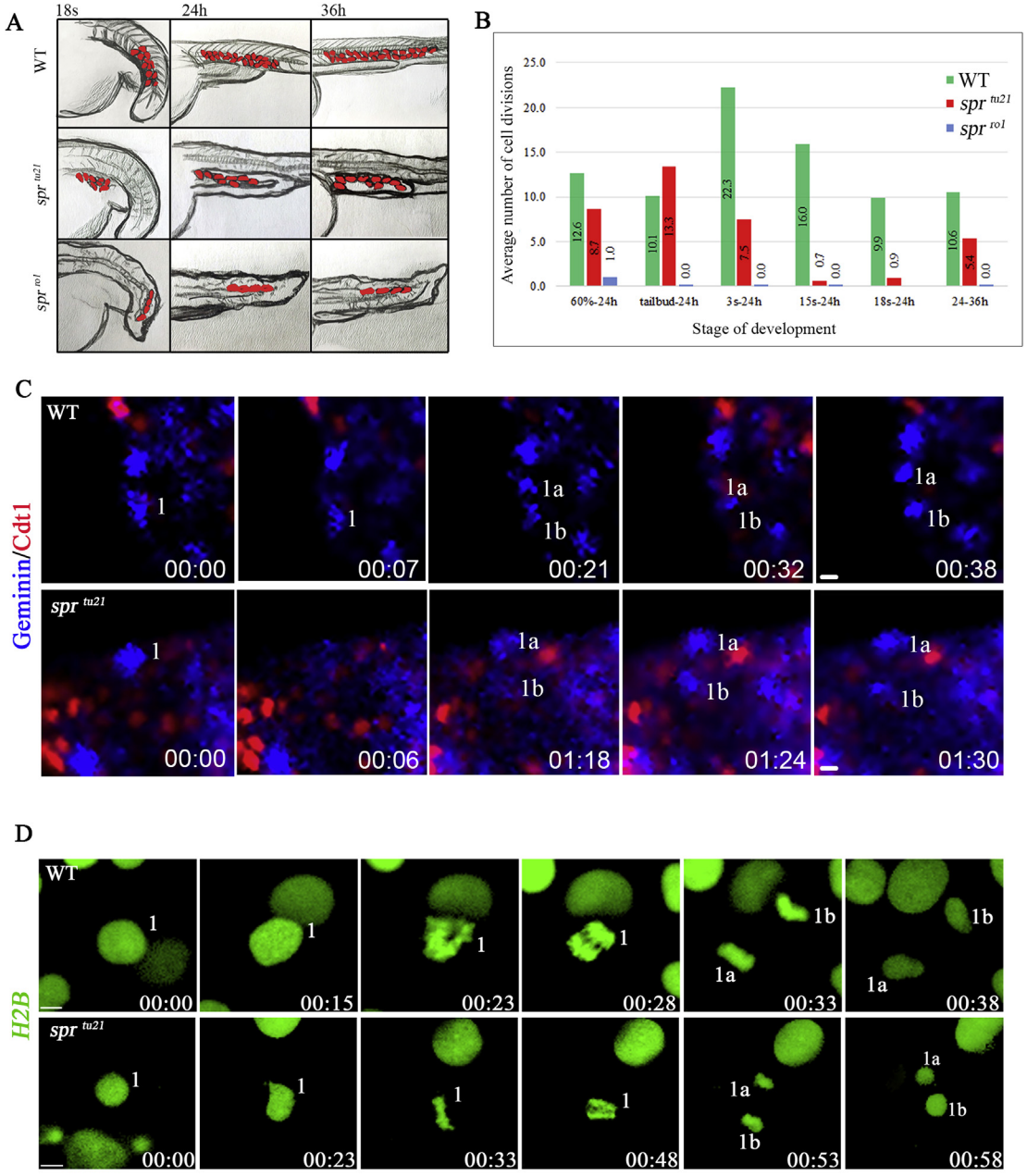

Fig. 6. Cell division does not completely stop in *spr* mutants; however, each allele has a unique phenotype. (A) Illustration of lineage tracing analysis for EVL cells in wild-type and mutant embryos. (B) Average number of cell divisions in a clone between the time marked and 24 h or 36 h. Each point is based on 3 or more clones. After tailbud, EVL cells cease to divide in the spr^{ro1} mutant. (C) Frames from a time-lapse recording, showing cell divisions still occur at 24 h in the EVL of wild-type embryos (top panel) and spr^{tu21} mutants (bottom panel). The Dual FUCCI transgene reports cells in the S/G2/early M phase of the cell cycle (blue) or in the G1 (G0) phase of cell cycle (red). Wild-type cells take approximately 20 minutes to go from metaphase to the next S-phase; whereas mutants take about 1 hour. Scale bar is 10 μm. (D) Frames from a time-lapse recording, showing that deep cells continue to divide at 5-somites (11.5 h) in wild-type embryos (top panel) and spr^{ro1} mutants (bottom panel) using *H2B-RFP* mRNA (pseudo colored in green) shows that wild-type cells take approximately 15 minutes to get through mitosis, whereas mutants take about 35 minutes. Scale bar is 5 μm.

development or *in vivo*. Here we show that the zebrafish mutant *specter* is a mutation in *cyclin B1*. Lack of zygotic Cyclin B1 does not prevent cells from entering new rounds of cell division. Rather, many mutant cells cycle more slowly and spend longer in G2 and M phases of the cell cycle and, of those, many enter apoptosis. We propose that although critical for a healthy timely division, other cell cycle proteins in part fulfil the function of Cyclin B1 to promote a cell through this portion of the cell cycle, suggesting fail safe mechanisms for this ancient conserved process.

4.1. The specter mutant is caused by a mutation in cyclin B1

We mapped the *spr* mutant to *cyclin B1*, sequenced the mutant gene and found a premature stop in exon 2 (Fig. 2). Rescue by the wild-type mRNA was not successful, possibly because there was not enough wild-type *cyclin B1* mRNA left by the time its translation is required, combined with the fact that Cyclin B1 protein is degraded every cell cycle (Brandeis et al., 1998). Our result is not unprecedented because similar attempts to rescue other cell cycle mutants in the laboratory, such as

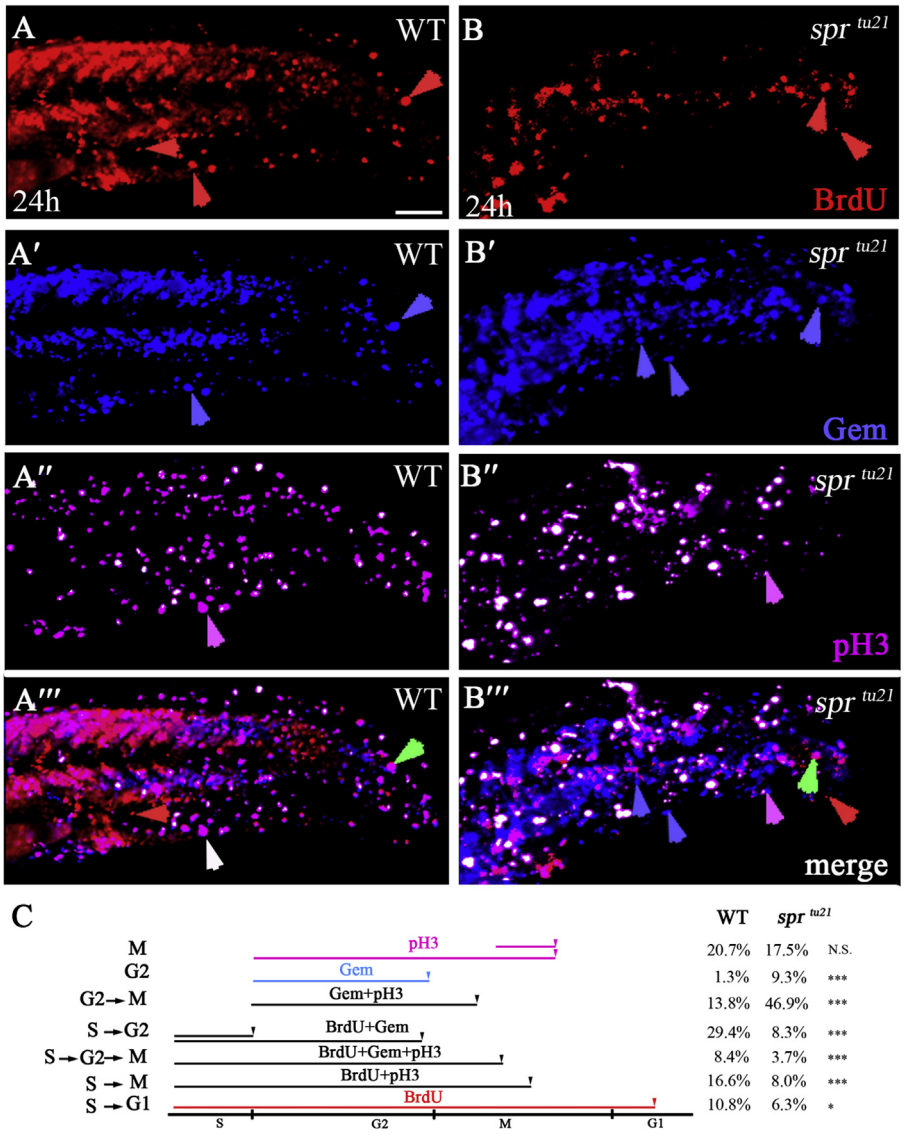

Fig. 7. *spr*^{tu21} mutant cells spend longer time in G2 and M phases. (A-B‴) The same cells in wild type (A-A‴) and mutant (B-B‴) visualized with different markers to distinguish between the stages of the cell cycle at 24 h. Embryos were labeled for 1 hour with BrdU and then fixed and stained for: anti-BrdU to visualize cells in the S-phase (A, B); anti-GFP to visualize Cerulean-Geminin cells in S/G2/early M phase (A′-B′); and anti-pH3 antibody to visualize cells in mitosis (A″, B″); or the merge (A‴, B‴). Symbols are: red arrows, cells that have gone through a full cell cycle and reside in G1 phase; green arrows, cells that have entered S phase; white arrows, cells that have gone through the S phase and entered mitosis; pink arrows, cells that have entered M phase but did not go through S phase; blue arrows, cells that have entered in the G2/early M phase. Scare bar is 50 μm. (C) Quantification of cells in a specific phase of the cell cycle from the data above.

zombie (Kane et al., 1996), have proved unsuccessful (unpublished). Where cell cycle mutants have been rescued, rescue was transient as rescue of *early mitotic inhibitor 1* mutants manifests during gastrulation and declines by tailbud suggesting that these synthetic transcripts are short lived (Zhang et al., 2008). In our case, the *specter* mutant phenotype is not visible, some two hours after gastrulation (Fig. 1). An alternative explanation for lack of rescue may be that the injected wild-type *cyclin B1* mRNA does not go through the necessary post-transcriptional modifications. Harvey et al. (2013) showed that polyadenylation of the *cyclin B1* 3′ UTR during early cleavage stages is highest during mitosis. Perhaps without a full 3′ UTR sequence the injected mRNA is not translated.

Making a CRISPR mutant that failed to complement *spr*^{tu21}, we confirmed *specter* is a mutation in *cyclin B1*. The CRISPR mutant is the result of a splice-site mutation which causes a gain-of-function phenotype (Figs. 3 and 5). Unlike the nonsense mutation, the CRISPR mutant displays zygotic expression of *cyclin B1*, suggesting that in the *spr*^{tu21} allele nonsense-mediated decay occurs, supporting that *spr*^{tu21} is a null mutation. However, even if its mRNAs were translated, the protein would only have a truncated chromatin localization domain (Pfaff and King, 2013), and no other essential domains (Bentley et al., 2007; Draviam et al., 2001; Pfaff and King, 2013). Together these data support the idea that *spr*^{tu21} is very likely a loss-of-function mutation in *cyclin B1*.

4.2. The ro1 allele causes a more severe phenotype than the null tu21 allele

We confirmed that *spr*^{tu21} is indeed a mutation in *cyclin B1* by creating a CRISPR mutant. Surprisingly, this new mutant has a more severe phenotype than the nonsense mutant. One hypothesis is that the *tu21* allele is a hypomorph, which seems unlikely because like many nonsense mutants its mRNA is degraded, and that the *ro1* allele is the null. Another hypothesis, however, is that the *ro1* allele is acting in a recessive gain-of-function fashion, blocking a compensatory mechanism when homozygous to overcome the G2/M arrest. We favor this explanation because although the *spr*^{ro1} mutant phenotype is more severe than the nonsense mutant, suggesting that it is a gain-of-function, it does not seem to have a dominant interfering effect when heterozygous like other similar cell cycle mutants in zebrafish such as *cellular island* (Yabe et al., 2009). Recessive gain-of-function mutations are not common, but in *C. elegans* and humans a number have been described. These include mutations in *degenerin* causing neuronal degeneration in *C. elegans* (García-Añoveros et al., 1995; reviewed by Lester and Karschin, 2000), and mutations in *BRDT*, a testis-specific gene, required for fertility in humans (Li et al., 2017). The products of these genes contribute to multimeric proteins, perhaps similar to Cyclin B1 which forms a complex with Cdk1 to create Mitosis Promoting Factor.

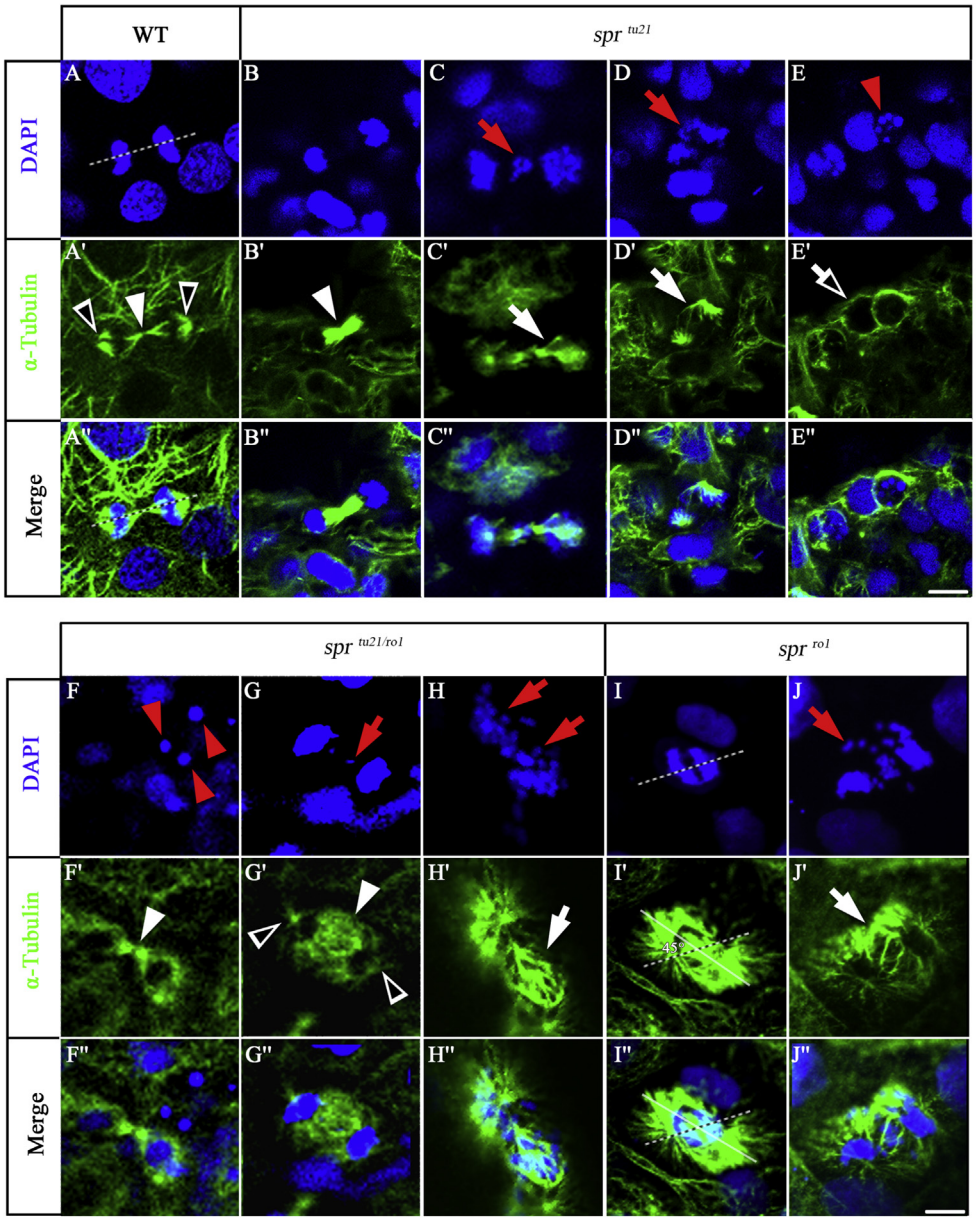

Fig. 8. *spr* mutants show signs of chromosome instability. DAPI staining and anti-alphaTubulin staining in the wild-type embryo (A-A″), the spr^{tu21} mutant (B-E″), $spr^{tu21/ro1}$ transheterozygote (F-H″), and the spr^{ro1} mutant (I-J″) at 24 h. Symbols are: red arrows, chromosome separation defects; red arrowheads, pyknotic nuclei suggestive of cell death; white arrowheads, polar microtubules; open white arrowheads, astral microtubules; open white arrows, apoptotic microtubules; white arrows, abnormal spindle microtubule organization; dashed line, expected spindle orientation; solid line, observed spindle orientation. Scale bar is 10 μm.

Notably, the spr^{ro1} mutant has an alternative splice site resulting in several different transcripts, one of which skips exons 2 through 5, remaining in frame (Fig. 4), and thus escaping nonsense-mediated degradation. Conceptual translation of this spr^{ro1} product would produce a Cyclin B1 protein missing a part of the chromatin localization domain, all of the destruction box, all of the cytoplasmic retention domain, and a part of the Cdk1-binding domain. This would cause Cyclin B1 to remain in the nucleus, while bound to Cdk1, and never getting ubiquitinated. Failure of degradation should prevent exit from the G2/M checkpoint, which would lead to apoptosis (Strauss et al., 2018). On the other hand, an abnormal Cdk1-binding domain might also prevent successful phosphorylation of nuclear caspases that prevent apoptosis (Allan and Clarke, 2007; Plaster et al., 2006). It is possible this interfering product outcompetes the wild-type maternal product once zygotic transcription begins, explaining perhaps its earlier phenotype. Regardless, in the *ro1* allele, by the end of gastrulation EVL cells no longer divide, and at early somite stages deep cells show signs of mitotic delay (Fig. 6). These observations suggest that maternal supplies are likely too depleted to sustain normal cell division some 12 hours later at 24 h (Fig. 8). $spr^{tu21/ro1}$ transheterozygote display similar phenotypes at 24 h (Fig. 8), where here as well abnormal Cyclin B1 would be produced. This, unlike the spr^{tu21} mutant, where lack of zygotic product can not interfere with any "potential" remaining maternal supplies.

4.3. Loss of zygotic Cyclin B1 slows the cell cycle but does not stop it

Maternal *cyclin B1* transcripts are present at least until the mid-blastula transition (Fig. 2D), providing the embryo with enough product to develop before zygotic transcription is activated (Kane and Kimmel, 1993). Many cell cycle mutants however, do not manifest a phenotype until the onset of gastrulation (6 h) (Kane et al., 1996; Riley et al., 2010; Song et al., 2004; Warga et al., 2016) some three or more cell cycles past the mid-blastula transition, suggesting that the expression of maternal transcripts sustain normal development up to this point. *specter* mutants, on the other hand, develop normally for longer until approximately 7-somites (12 h), although this time varies and can be much later. However, even after 24 h, cells still cycle, although the majority of cells are predominantly in the G2 or M phase of the cell cycle, indicating that

cells are delayed in these phases (Fig. 7). Therefore, it seems possible that maternal input of *cyclin B1* at a very low level sustains normal development well into somitogenesis, but once this threshold falls, the cell cycle is compromised.

This is consistent with observations in the *crash-and-burn* mutant, carrying a mutation in the Mybl2b transcription factor (formerly known as b-Myb), where cells also show signs of delayed mitosis by 15-somites (Shepard et al., 2005). Mybl2b regulates progression through the G1 to S phases of the cell cycle, and indirectly, progression through the G2 to M phase of the cell cycle by upregulating *cyclin B1*. Knockdown of *mybl2b* results in reduction of Cyclin B1 and Cdk1 expression (Okada et al., 2002; Shepard et al., 2005). Like in the *spr* mutant, cells in the *crash-and-burn* mutant exhibit abnormal mitotic spindles and unseparated chromosomes (Shepard et al., 2005; Stern et al., 2005), however, unlike cells in the *spr* mutant, none of these cells escape mitotic arrest and cell death likely because of the absence of Mybl2b has far more severe effects on the cell cycle.

Why does lack of Cyclin B1 stop cell division in the mouse but not in zebrafish? Perhaps in zebrafish, low levels of maternal *cyclin B1* transcripts generate enough protein to sustain cell divisions well up to 24 h, occluding the true loss-of-function phenotype. However, because Cyclin B1 is degraded after each cell cycle (Brandeis and Hunt, 1996; Clute and Pines, 1999), over time there would eventually be no more Cyclin B1 once maternal transcripts are degraded. Whether this happens by early somite stages, like most cell cycle genes (Riley et al., 2010; Song et al., 2004; Warga et al., 2016), is unclear, but unlike *cyclin A* and *cyclin B2,* degradation of maternal *cyclin B1* is not zygotically regulated (Audic et al., 2001). Thus, even in the absence of a zygotic product like in the *tu21* allele or the expression of an altered zygotic product like in the *ro1* allele, maternal Cyclin B1 should clear normally, and most likely before 24 h.

Hence, we hypothesize that in zebrafish, another cell cycle protein partially compensates for the absence of zygotic Cyclin B1. We know that *cyclin B2* mRNA is expressed maternally, and is ubiquitously distributed throughout both, wild type and spr^{tu21} mutants at 24 h (T.P. unpublished). Although current research in mouse shows little support for the Cyclin B2 regulating the G2 to M transition (Strauss et al., 2018), in human culture cells, Cyclin B2 partially compensates for absence of Cyclin B1 by forming an active MPF with Cdk1 (Bellanger et al., 2007). Therefore, it is possible in zebrafish that Cyclin B2 compensates for Cyclin B1 to promote cell divisions in response to G2/M arrest. A further possibility is that Cyclin A compensates for lack of Cyclin B1 as is observed in human culture cell studies (Gong et al., 2010) (Fig. 9). However, it should be noted that some mutant cells undergo successful rounds of cell division, not all cells overcome lack of endogenous Cyclin B1. This suggests a compensatory mechanism that is only partly effective, and not sufficient for a completely normal cell cycle. This is in agreement with previous studies on Cyclin B1 deficient cells in human culture cell studies where cells show persistent lagging chromosomes and delayed mitosis (Knoblich and Lehner, 1993; Nam and Van Deursen, 2014). We also hypothesize that only when Cdk1 is prevented from binding to any factor is the cell cycle really stopped (Fig. 9) as is seen, for the most part, in the spr^{ro1} allele.

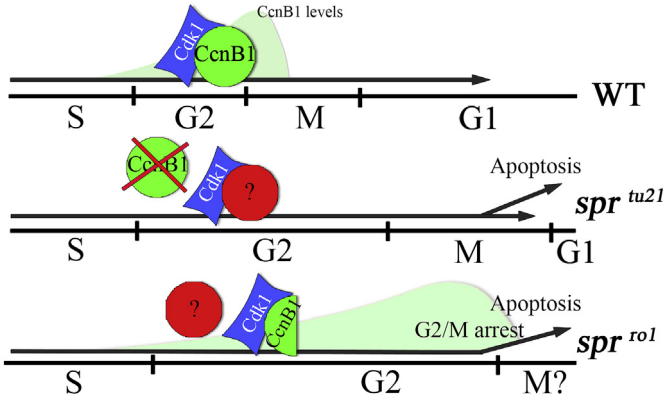

Fig. 9. Model of cell cycle progression in wild-type, spr^{tu21} and spr^{ro1} mutants. Cyclin B1 (CcnB1) forms an active mitosis promoting factor (MPF) with Cdk1 at the end of the G2 phase as the Cyclin B1 threshold is reached. This complex is then translocated to the nucleus to overcome the G2/M checkpoint and allow entry into mitosis in wild type (WT). In the absence of functional zygotic Cyclin B1 (spr^{tu21}), the transition though the G2/M checkpoint still occurs. Perhaps because another cell cycle protein forms a partly functional MPF with Cdk1, allowing cells to divide. However, mitosis takes longer occasional with chromosomal instability and subsequent apoptosis. In contrast, in the presence of an altered Cyclin B1 protein (spr^{ro1}), MPF forms, preventing other proteins from binding to Cdk1, but this MPF is not functional and cells arrest at the G2/M checkpoint or undergo apoptosis once maternal supplies of wild-type Cyclin B1 are depleted.

In summary, we show that Cyclin B1 is essential for normal cell cycle progression. Yet lack of zygotic Cyclin B1 does not prevent cells from dividing as expected, stopping them at the G2/M checkpoint. Instead, cells slow down and continue to divide. Hence, our data argues there may be more players than Cyclin B1 to coordinate mitotic entry in keeping with the redundancy often seen in ancient conserved processes. In our future work, we will examine the possibility that Cyclin B2 is one of those players.

Acknowledgements

We thank David Kimelman for the gift of the Dual FUCCI transgenic zebrafish, Keith Joung for the gift of the DR274 plasmid, Lilianna Solnica-Krezel and Diane Sepich for the *H2B-RFP* plasmid and Mark Webster for assistance with BrdU labeling. We would also like to thank Kane lab members, as well as Pam Hoppe, Todd Barkman, and Wendy Beane for constructive comments and patience. This work was supported by NSF grant (1022347) to D.A.K. and a FRAACA award W2015-024 from Western Michigan University, as well as a Fulbright Graduate Student grant to Tetiana Petrachkova.

Appendix A. Supplementary data

Supplementary data to this article can be found online at https://doi.org/10.1016/j.ydbio.2019.03.014.

References

Abe, T., Sakaue-Sawano, A., Kiyonari, H., Shioi, G., Inoue, K. -i., Horiuchi, T., Nakao, K., Miyawaki, A., Aizawa, S., Fujimori, T., 2013. Visualization of cell cycle in mouse embryos with Fucci2 reporter directed by Rosa 26 promoter. Development 140, 237–246. https://doi.org/10.1242/dev.084111.

Allan, L.A., Clarke, P.R., 2007. Phosphorylation of caspase-9 by CDK1/cyclin B1 protects mitotic cells against apoptosis. Mol. Cell 26, 301–310. https://doi.org/10.1016/j.molcel.2007.03.019.

Audic, Y., Anderson, C., Bhatty, R., Hartley, R.S., 2001. Zygotic regulation of maternal Cyclin A1 and B2 mRNAs. Mol. Cell Biol. 21, 1662–1671. https://doi.org/10.1128/MCB.21.5.1662-1671.2001.

Bellanger, S., De Gramont, A., Sobczak-Thépot, J., 2007. Cyclin B2 suppresses mitotic failure and DNA re-replication in human somatic cells knocked down for both cyclins B1 and B2. Oncogene 26, 7175–7184. https://doi.org/10.1038/sj.onc.1210539.

Bennett, C.M., Kanki, J.P., Rhodes, J., Liu, T.X., Paw, B.H., Kieran, M.W., Langenau, D.M., Delahaye-brown, A., Zon, L.I., Fleming, M.D., Look, A.T., 2001. Myelopoiesis in the zebrafish. Danio rerio 98, 643–651. https://doi.org/https://doi.org/10.1182/blood.V98.3.643.

Bentley, A.M., Normand, G., Hoyt, J., King, R.W., Salmon, T., 2007. Distinct sequence Elements of cyclin B1 promote localization to chromatin, centrosomes, and kinetochores during mitosis. Mol. Biol. Cell 18, 4847–4858. https://doi.org/10.1091/mbc.e06-06-0539.

Bouldin, C.M., Kimelman, D., 2014. Dual fucci: a new transgenic line for studying the cell cycle from embryos to adults. Zebrafish 11, 182–183. https://doi.org/10.1089/zeb.2014.0986.

Brandeis, M., Hunt, T., 1996. The proteolysis of mitotic cyclins in mammalian cells persists from the end of mitosis until the onset of S phase. EMBO J. 15, 5280–5289.

Brandeis, M., Rosewell, I., Carrington, M., Crompton, T., Jacobs, M.A., Kirk, J., Gannon, J., Hunt, T., 1998. Cyclin B2-null mice develop normally and are fertile

whereas cyclin B1-null mice die in utero. Proc. Natl. Acad. Sci. 95, 4344–4349. https://doi.org/10.1073/pnas.95.8.4344.
Brownlie, A., Donovan, A., Pratt, S.J., Paw, B.H., Oates, A.C., Brugnara, C., Witkowska, H.E., Sassa, S., Zon, L.I., 1998. Positional cloning of the zebrafish sauternes gene: a model for congenital sideroblastic anaemia. Nat. Genet. 20, 244–250. https://doi.org/10.1038/3049.
Clijsters, L., Ogink, J., Wolthuis, R., 2013. The spindle checkpoint, APC/CCdc 20, and APC/CCdh1 play distinct roles in connecting mitosis to S phase. J. Cell Biol. 201, 1013–1026. https://doi.org/10.1083/jcb.201211019.
Clute, P., Pines, J., 1999. Temporal and spatial control of cyclin B1 destruction in metaphase. Nat. Cell Biol. 1, 82–87. https://doi.org/10.1038/10049.
Daldello, E.M., Luong, X.G., Yang, C.-R., Huhn, J., Conti, M., 2018. Cyclin B2 is required for progression through meiosis in mouse oocytes. bioRxiv, 441352. https://doi.org/10.1101/441352.
Draetta, G., Luca, F., Westendorf, J., Brizuela, L., Ruderman, J., Beach, D., 1989. cdc 2 protein kinase is complexed with both cyclin A and B: evidence for proteolytic inactivation of MPF. Cell 56, 829–838. https://doi.org/https://doi.org/10.1016/0092-8674(89)90687-9.
Draviam, V.M., Orrechia, S., Lowe, M., Pardi, R., Pines, J., 2001. The localization of human cyclins B1 and B2 determines CDK1 substrate specificity and neither enzyme requires MEK to disassemble the Golgi apparatus. J. Cell Biol. 152, 945–958. https://doi.org/10.1083/jcb.152.5.945.
Gallant, P., Nigg, E.A., 1994. Identification of a novel vertebrate cyclin: cyclin B3 shares properties with both A- and B-type cyclins. EMBO J. 13, 595–605. https://doi.org/10.1002/J.1460-2075.1994.TB06297.X.
Gallant, P., Nigg, E.A., 1992. Cyclin B2 undergoes cell cycle-dependent nuclear translocation and, when expressed as a non-destructible mutant, causes mitotic arrest in HeLa cells. J. Cell Biol. 117, 213–224. https://doi.org/10.1083/jcb.117.1.213.
García-Añoveros, J., Ma, C., Chalfie, M., 1995. Regulation of Caenorhabditis elegans degenerin proteins by a putative extracellular domain. Curr. Biol. 5, 441–448. https://doi.org/10.1016/S0960-9822(95)00085-6.
Gavet, O., Pines, J., 2010. Activation of cyclin B1-Cdk1 synchronizes events in the nucleus and the cytoplasm at mitosis. J. Cell Biol. 189, 247–259. https://doi.org/10.1083/jcb.200909144.
Gong, D., Ferrell, J.E., Lew, D.J., 2010. The roles of cyclin A2, B1, and B2 in early and late mitotic events. Mol. Biol. Cell 21, 3149–3161. https://doi.org/10.1091/mbc.e10-05-0393.
Gui, L., Homer, H., 2013. Article regulates the G2-M transition and early prometaphase in mouse oocytes. Dev. Cell 25, 43–54. https://doi.org/10.1016/j.devcel.2013.02.008.
Haffter, P., Granato, M., Brand, M., Mullins, M.C., Hammerschmidt, M., Kane, D.A., Odenthal, J., van Eeden, F.J., Jiang, Y.J., Heisenberg, C.P., Kelsh, R.N., Furutani-Seiki, M., Vogelsang, E., Beuchle, D., Schach, U., Fabian, C., Nusslein-Volhard, C., 1996. The identification of genes with unique and essential functions in the development of the zebrafish, Danio rerio. Development 123, 1–36.
Harvey, S.A., Sealy, I., Kettleborough, R., Fenyes, F., White, R., Stemple, D., Smith, J.C., 2013. Identification of the zebrafish maternal and paternal transcriptomes. Development 140, 2703–2710. https://doi.org/10.1242/dev.095091.
Hendzel, M.J., Wei, Y., Mancini, M.A., Van Hooser, A., Ranalli, T., Brinkley, B.R., Bazett-Jones, D.P., Allis, C.D., 1997. Mitosis-specific phosphorylation of histone H3 initiates primarily within pericentromeric heterochromatin during G2 and spreads in an ordered fashion coincident with mitotic chromosome condensation. Chromosoma 106, 348–360. https://doi.org/10.1007/s004120050256.
Herbomel, P., Thisse, B., Thisse, C., 1999. Ontogeny and behaviour of early macrophages in the zebrafish embryo. Development 126, 3735–3745.
Hochegger, H., Takeda, S., Hunt, T., 2008. Cyclin-dependent kinases and cell-cycle transitions: does one fit all? Nat. Rev. Mol. Cell Biol. 9, 910–916. https://doi.org/10.1038/nrm2510.
Hwang, W.Y., Fu, Y., Reyon, D., Maeder, M.L., Tsai, S.Q., Sander, J.D., Peterson, R.T., Yeh, J.R.J., Joung, J.K., 2013. Efficient genome editing in zebrafish using a CRISPR-Cas system. Nat. Biotechnol. 31, 227–229. https://doi.org/10.1038/nbt.2501.
Ikegami, R., Hunter, P., Yager, T.D., 1999. Developmental activation of the capability to undergo checkpoint- induced apoptosis in the early zebrafish embryo. Dev. Biol. 209, 409–433. https://doi.org/10.1006/dbio.1999.9243.
Jackman, M., Lindon, C., Niggt, E.A., Pines, J., 2003. Active cyclin B1-Cdk1 first appears on centrosomes in prophase. Nat. Cell Biol. 5, 143–148. https://doi.org/10.1038/ncb918.
Johnson, S.L., Africa, D., Home, S., Postlethwait, J.H., 1995. Half-tetrad analysis in zebrafish: mapping the ros mutation and the centromere of Linkage Group I. Genetics 139, 1727–1735.
Kane, D.A., Kimmel, C.B., 1993. The zebrafish midblastula transition. Development 119, 447–456.
Kane, D.A., Maischein, H.M., Brand, M., van Eeden, F.J., Furutani-Seiki, M., Granato, M., Haffter, P., Hammerschmidt, M., Heisenberg, C.P., Jiang, Y.J., Kelsh, R.N., Mullins, M.C., Odenthal, J., Warga, R.M., Nüsslein-Volhard, C., 1996. The zebrafish early arrest mutants. Development 123, 57–66.
Kimmel, C.B., Warga, R.M., Kane, D.A., 1994. Cell cycles and clonal strings during formation of the zebrafish central nervous system. Development 120, 265–276.
Kimmel, C.B., Warga, R.M., Schilling, T.F., 1990. Origin and organization of the zebrafish fate map. Development 108, 581–594.
Kimura, K., Hirano, M., Kobayashi, R., Hirano, T., 1998. Phosphorylation and activation of 13S condensin by Cdc2 in vitro. Science (80-.) 282, 487–490. https://doi.org/10.1126/science.282.5388.487.
Knapik, E.W., Goodman, A., Ekker, M., Chevrette, M., Delgado, J., Neuhauss, S., Shimoda, N., Driever, W., Fishman, M.C., Jacob, H.J., 1998. A microsatellite genetic linkage map for zebrafish (Danio rerio). Nat. Genet. 18, 338–343.
Knoblich, J.A., Lehner, C.F., 1993. Synergistic action of Drosophila cyclins A and B during the G2-M transition. EMBO J. 12, 65–74. https://doi.org/10.1002/j.1460-2075.1993.tb05632.x.
Kotani, T., Yoshida, N., Mita, K., Yamashita, M., 2001. Requirement of cyclin B2 , but not cyclin B1 , for bipolar spindle formation in frog (Rana japonica) oocytes. Mol. Reprod. Dev. 208, 199–208. https://doi.org/10.1002/mrd.1023.
Kreutzer, M.A., Richards, J.P., De Silva-Udawatta, M.N., Temenak, J.J., Knoblich, J.A., Lehner, C.F., Bennett, K.L., 1995. Caenorhabditis elegans cyclin A- and B-type genes: a cyclin A multigene family, an ancestral cyclin B3 and differential germline expression. J. Cell Sci. 108, 2415–2424.
Lester, H.A., Karschin, A., 2000. Gain of function mutants: ion channels and G protein-coupled receptors. Annu. Rev. Neurosci. 23, 89–125.
Li, J., Tang, J.-X., Cheng, J.-M., Hu, B., Wang, Y.-Q., Aalia, B., Li, X.-Y., Jin, C., Wang, X.-X., Deng, S.-L., Zhang, Y., Chen, S.-R., Qian, W.-P., Sun, Q.-Y., Huang, X.-X., Liu, Y.-X., 2018. Cyclin B2 can compensate for Cyclin B1 in oocyte meiosis I. J. Cell Biol. 217, 3901. LP-3911. https://doi.org/10.1083/jcb.201802077.
Li, L., Sha, Y., Wang, X., Li, P., Wang, J., Kee, K., Wang, B., 2017. Whole-exome sequencing identified a homozygous BRDT mutation in a patient with acephalic spermatozoa. Oncotarget 8, 19914–19922. https://doi.org/10.18632/oncotarget.15251.
Lieschke, G.J., Oates, A.C., Crowhurst, M.O., Ward, A.C., Layton, J.E., 2001. Morphologic and functional characterization of granulocytes and macrophages in embryonic and adult zebrafish. Blood 98, 3087–3096.
Lindqvist, A., Rodríguez-Bravo, V., Medema, R.H., 2009. The decision to enter mitosis: feedback and redundancy in the mitotic entry network. J. Cell Biol. 185, 193–202. https://doi.org/10.1083/jcb.200812045.
Liu, Y., Sepich, D.S., Solnica-Krezel, L., 2017. Stat 3/Cdc25a-dependent cell proliferation promotes embryonic axis extension during zebrafish gastrulation. PLoS Genet. 13, 1–32. https://doi.org/10.1371/journal.pgen.1006564.
McFarland, K.N., Warga, R.M., Kane, D.A., 2005. Genetic locus half baked is necessary for morphogenesis of the ectoderm. Dev. Dynam. 233, 390–406. https://doi.org/10.1002/dvdy.20325.
Minshull, J., Pines, J., Golsteyn, R., Standart, N., Mackie, S., Colman, A., Blow, J., Ruderman, J.V., Wu, M., Hunt, T., 1989. The role of cyclin synthesis, modification and destruction in the control of cell division. J. Cell Sci. Suppl. 12, 77–97. https://doi.org/10.1242/jcs.1989.Supplement_12.8.
Moss, D.K., Betin, V.M., Malesinski, S.D., Lane, J.D., 2006. A novel role for microtubules in apoptotic chromatin dynamics and cellular fragmentation. J. Cell Sci. 119, 2362–2374. https://doi.org/10.1242/jcs.02959.
Nam, H.J., Van Deursen, J.M., 2014. Cyclin B2 and p53 control proper timing of centrosome separation. Nat. Cell Biol. 16, 535–546. https://doi.org/10.1038/ncb2952.
Negron, J.F., Lockshin, R.A., 2004. Activation of apoptosis and caspase-3 in zebrafish early gastrulae. Dev. Dynam. 231, 161–170. https://doi.org/10.1002/dvdy.20124.
Nieduszynski, C.A., Murray, J., Carrington, M., 2002. Whole-genome analysis of animal A- and B-type cyclins. Genome Biol. 3. https://doi.org/10.1186/gb-2002-3-12-research0070.
Nigg, E.A., 2001. Mitotic kinases as regulators of cell division and its checkpoints. Nat. Rev. Mol. Cell Biol. 2, 21–32. https://doi.org/10.1038/35048096.
Okada, M., Akimaru, H., Hou, D., Takahashi, T., Ishii, S., 2002. Myb controls G 2/M progression by inducing cyclin B expression in the Drosophila eye imaginal disc. EMBO J. 21, 675–684.
Oxtoby, E., Jowett, T., 1993. Cloning of the zebrafish krox-20 gene (krx-20) and its expression during hindbrain development. Nucleic Acids Res. 21, 1087–1095. https://doi.org/10.1093/nar/21.5.1087.
Pfaff, K.L., King, R.W., 2013. Determinants of human cyclin B1 association with mitotic chromosomes. PLoS One 8. https://doi.org/10.1371/journal.pone.0059169.
Phillips, B.T., Kwon, H.J., Melton, C., Houghtaling, P., Fritz, A., Riley, B.B., 2006. Zebrafish msxB, msxC and msxE function together to refine the neural-nonneural border and regulate cranial placodes and neural crest development. Dev. Biol. 294, 376–390. https://doi.org/10.1016/j.ydbio.2006.03.001.
Pines, J., 1995. Cyclins and cyclin-dependent kinases: a biochemical view. Biochem. J. 308, 697–711. https://doi.org/10.1042/bj3080697.
Pines, J., Hunter, T., 1989. Isolation of a human cyclin cDNA: evidence for cyclin mRNA and protein regulation in the cell cycle and for interaction with p34cdc 2. Cell 58, 833–846. https://doi.org/10.1016/0092-8674(89)90936-7.
Plaster, N., Sonntag, C., Busse, C.E., Hammerschmidt, M., 2006. p53 deficiency rescues apoptosis and differentiation of multiple cell types in zebrafish flathead mutants deficient for zygotic DNA polymerase δ1. Cell Death Differ. 13, 223–235. https://doi.org/10.1038/sj.cdd.4401747.
Porter, L.A., Donoghue, D.J., 2003. Cyclin B1 and CDK1: nuclear localization and upstream regulators. Prog. Cell Cycle Res. 5, 335–347.
Riley, B.B., Sweet, E.M., Heck, R., Evans, A., McFarland, K.N., Warga, R.M., Kane, D.A., 2010. Characterization of harpy/Rca1/emi 1 mutants: patterning in the absence of cell division. Dev. Dynam. 239, 828–843. https://doi.org/10.1002/dvdy.22227.
Santamaría, D., Barrière, C., Cerqueira, A., Hunt, S., Tardy, C., Newton, K., Cáceres, J.F., Dubus, P., Malumbres, M., Barbacid, M., 2007. Cdk1 is sufficient to drive the mammalian cell cycle. Nature 448, 811–815. https://doi.org/10.1038/nature06046.
Shepard, J.L., Amatruda, J.F., Stern, H.M., Subramanian, A., Finkelstein, D., Ziai, J., Finley, K.R., Pfaff, K.L., Hersey, C., Zhou, Y., Barut, B., Freedman, M., Lee, C., Spitsbergen, J., Neuberg, D., Weber, G., Golub, T.R., Glickman, J.N., Kutok, J.L., Aster, J.C., Zon, L.I., 2005. A zebrafish bmyb mutation causes genome instability and increased cancer susceptibility. Proc. Natl. Acad. Sci. 102, 13194–13199. https://doi.org/10.1073/pnas.0506583102.

Siefert, J.C., Clowdus, E.A., Sansam, C.L., 2015. Cell cycle control in the early embryonic development of aquatic animal species. Comp. Biochem. Physiol. Part C Toxicol. Pharmacol. 178, 8–15. https://doi.org/10.1016/j.cbpc.2015.10.003.

Song, M.H., Brown, N.L., Kuwada, J.Y., 2004. The cfy mutation disrupts cell divisions in a stage-dependent manner in zebrafish embryos. Dev. Biol. 276, 194–206. https://doi.org/10.1016/j.ydbio.2004.08.041.

Stern, H.M., Murphey, R.D., Shepard, J.L., Amatruda, J.F., Straub, C.T., Pfaff, K.L., Gerhard, W., Tallarico, J.A., King, R.W., Zon, L.I., 2005. Small molecules that delay s phase suppress a zebrafish bmyh mutant. Nat. Chem. Biol. 1, 366–370. https://doi.org/10.1038/nchembio749.

Strauss, B., Harrison, A., Coelho, P.A., risata, K., Zernicka-Goetz, M., Pines, J., 2018. Cyclin B1 is essential for mitosis in mouse embryos, and its nuclear export sets the time for mitosis. J. Cell Biol. 217, 179–193. Yfile:///C:/Users/Vadim/Desktop/Lab/references/cyclin-b2-is-required-for-progression-through-meiosis-in-mouse-oocytes. https://doi.org/10.1083/jcb.201612147.

Streisinger, G., Singer, F., Walker, C., Knauber, D., Dower, N., 1986. Segregation analyses and gene-centromere distances in zebrafish. Genetics 112, 311–319.

Sugimoto, N., Tatsumi, Y., Tsurumi, T., Matsukage, A., Kiyono, T., Nishitani, H., Fujita, M., 2004. Cdt1 phosphorylation by cyclin A-dependent kinases negatively regulates its function without affecting Geminin binding. J. Biol. Chem. 279, 19691–19697. https://doi.org/10.1074/jbc.M313175200.

Sugiyama, M., Sakaue-Sawano, A., Iimura, T., Fukami, K., Kitaguchi, T., Kawakami, K., Okamoto, H., Higashijima, S. -i., Miyawaki, A., 2009. Illuminating cell-cycle progression in the developing zebrafish embryo. Proc. Natl. Acad. Sci. 106, 20812–20817. https://doi.org/10.1073/pnas.0906464106.

Thisse, C., Thisse, B., 2008. High-resolution in situ hybridization to whole-mount zebrafish embryos. Nat. Protoc. 3, 59–69. https://doi.org/10.1038/nprot.2007.514.

Unhavaithaya, Y., Park, E.A., Royzman, I., Orr-Weaver, T.L., 2013. Drosophila embryonic cell-cycle mutants. Genetics 3, 1875–1880. https://doi.org/10.1534/g3.113.007880.

Warga, R.M., Kane, D.A., 2003. One-eyed pinhead regulates cell motility independent of Squint/Cyclops signaling. Dev. Biol. 261, 391–411. https://doi.org/10.1016/S0012-1606(03)00328-2.

Warga, R.M., Kane, D.A., Ho, R.K., 2009. Fate mapping embryonic blood in zebrafish: multi- and unipotential lineages are segregated at gastrulation. Dev. Cell 16, 744–755. https://doi.org/10.1016/j.devcel.2009.04.007.

Warga, R.M., Nüsslein-Volhard, C., 1999. Origin and development of the zebrafish endoderm. Development 126, 827–838.

Warga, R.M., Wicklund, A., Webster, S.E., Kane, D.A., 2016. Progressive loss of RacGAP1/ogre activity has sequential effects on cytokinesis and zebrafish development. Dev. Biol. 418, 307–322. https://doi.org/10.1016/j.ydbio.2016.06.021.

Yabe, T., Ge, X., Lindeman, R., Nair, S., Runke, G., Mullins, M.C., Pelegri, F., 2009. The maternal-effect gene cellular island encodes aurora B kinase and is essential for furrow formation in the early zebrafish embryo. PLoS Genet. 5, e1000518. https://doi.org/https://doi.org/10.1371/journal.pgen.1000518.

Zachariae, W., Nasmyth, K., 1999. Whose end is destruction: cell division and the anaphase- promoting complex. Genes Dev. 13, 2039–2058. https://doi.org/10.1101/gad.13.16.2039.

Zhang, L., Kendrick, C., Julich, D., Holley, S.A., 2008. Cell cycle progression is required for zebrafish somite morphogenesis but not segmentation clock function. Development 135, 2065–2070. https://doi.org/10.1242/dev.022673.